Reply to anonymous referee #1

Dear referee,

We appreciate your valuable questions and comments on our manuscript. The point-by-point answers to the questions and comments are listed as follows.

Your sincerely,

Jianrong Zhu, on behalves of the co-authors

Comment 1: Section 2.1: It can be seen from observed salinity (in Figure 2a) that at normal condition the salinity at the upstream Chongxi station is higher than other stations, while during the abnormal condition (i.e., the studied case) the maximum salinity concentration appears at Baozhen station. I would suggest the authors to clarify the difference between these two conditions since the underlying mechanism for saltwater intrusion may be completely different. For instance, to what extent the spilling of saltwater from the North Branch into the South Branch may impact the dynamics of saltwater concentration during this abnormal condition when compared with the normal condition.

Reply: Thanks for your good comment. At normal condition with climatic wind in dry season, there exits the saltwater-spill-over (SSO) from the North Branch into the South Branch in spring tide that results in the salinity at Chongxi station is higher than at Nanmen and Baozhen stations. While during the abnormal condition with persistent and strong northerly wind in February 2014, the maximum salinity was greatly higher at Baozhen station than at Chongxi station. In order to quantitative analysis of impact of the SSO on the saltwater intrusion in the South Branch, the temporal variations in residual water flux and salt flux across sec2 (labeled in Figure 1) at the upper reaches of the North Branch in February, 2014 were added under climatic wind and real wind in February 2014. In addition, a numerical experiment in which the upper reaches of the North Branch is blocked was designed to distinguish how much effect of the SSO on saltwater intrusion in the South Branch under the real wind in February 2014. The above contents are added in the discussion section 4.1 in the

revised manuscript.

In the original manuscript, we did not mention the SSO. Now we added the description of SSO at the end of the third paragraph in introduction section: The most characteristic type of saltwater intrusion in the estuary is the saltwater-spill-over (SSO) from the North Branch into the South Branch (Shen et al., 2003; Wu et al., 2006; Lyu and Zhu, 2018). The shallow and funnel-shaped topography help to prevent runoff from entering the North Branch, especially during the dry season, and makes the tidal range larger in the North Branch than in the South Branch. The saltwater from the SSO is transported downstream by runoff and arrives in the middle reaches of the South Branch during the subsequent neap tide and threatens the water supplies of reservoirs located in the estuary.

Comment 2: Section 2.1: With regard to this section, I would suggest to move the analysis of the observed data into "Results" section 3.

Reply: Thanks. We moved the Section 2.1 into "Results" section 3.1 in the revised manuscript. The relevant section number was changed.

Comment 3: Calibration and Validation of the numerical model: Although the saltwater intrusion model has been extensively calibrated and validated, I would suggest the authors to present the calibration for the salinity along the channel (i.e., Baozhen, Nanmen, Chongxi and Qingcaosha). For the time being, we can only see the reproduction of the salinity in Baozhen station, while the performances in other available stations are unknown. In addition, it would be better to clarify the basic calibration parameters used in the numerical model in the manuscript.

Reply: It's a very good suggestion. In order to save the length of the original manuscript, we only presented the model validation for the salinity at Baozhen station. We first calibrated the model for water level and salinity by adjusting the basic parameters of bottom drag coefficient, vertical turbulent viscosity and diffusion coefficient used in the numerical model, then validated the model. Now we added the model validation for salinity at Baozhen, Nanmen, Chongxi and Qingcaosha stations

long the channel in Figure 3, and for water level at Baozhen, Sheshan and Luchaogang stations in Figure 6.

Because the model validation for salinity and water level at the hydrologic stations were added, the figures in the original manuscript were renumbered and redrew. Other figures are listed at the end of the reply.

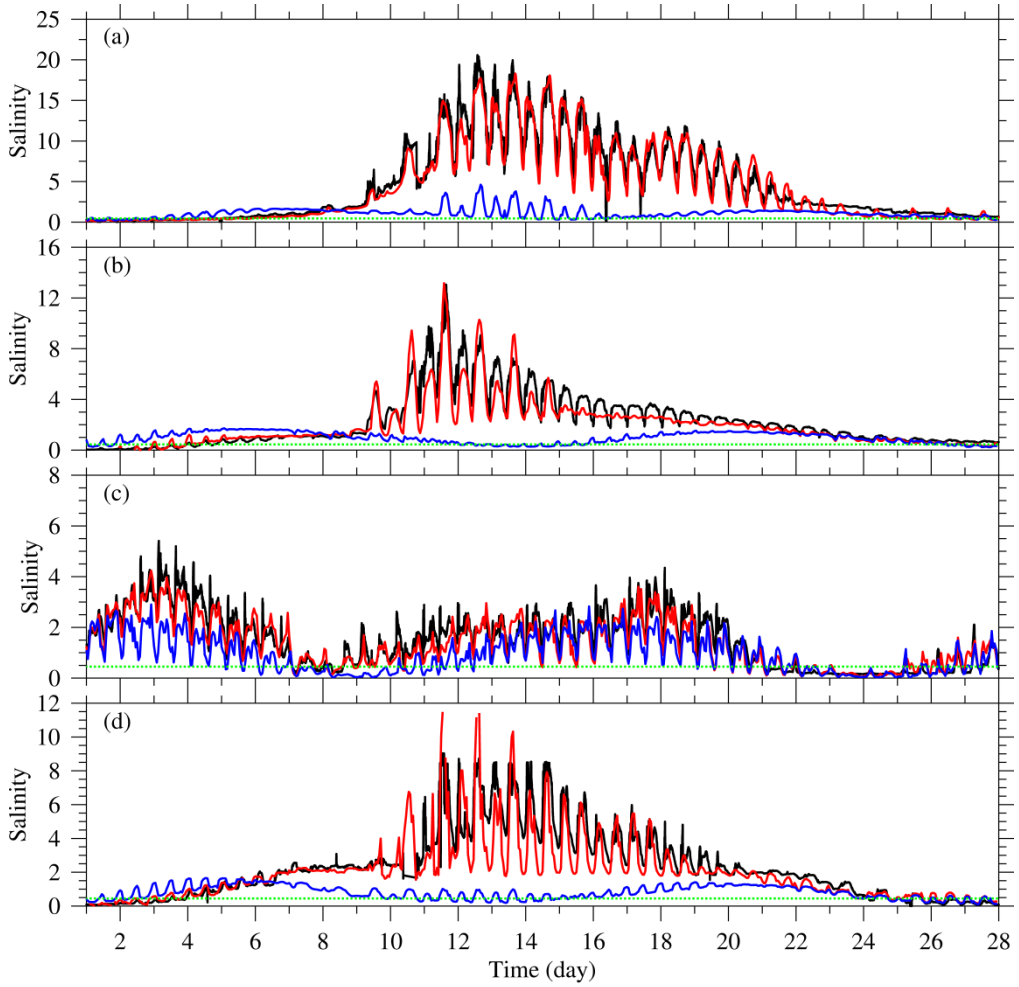

Figure 3: Temporal variations in salinity in February 2014 at hydrologic stations. a: Baozhen station; b: Nanmen station; c: Chongxi station; c: Qingcaosha station. Black line: measured salinity; blue line: simulated salinity under climatic wind and residual water level conditions at open sea boundaries (Exp 1); red line: simulated salinity under a realistic wind and residual water levels at the open sea boundaries (Exp 2). The dashed green line represents salinity of 0.45, which is the standard for drinking water.

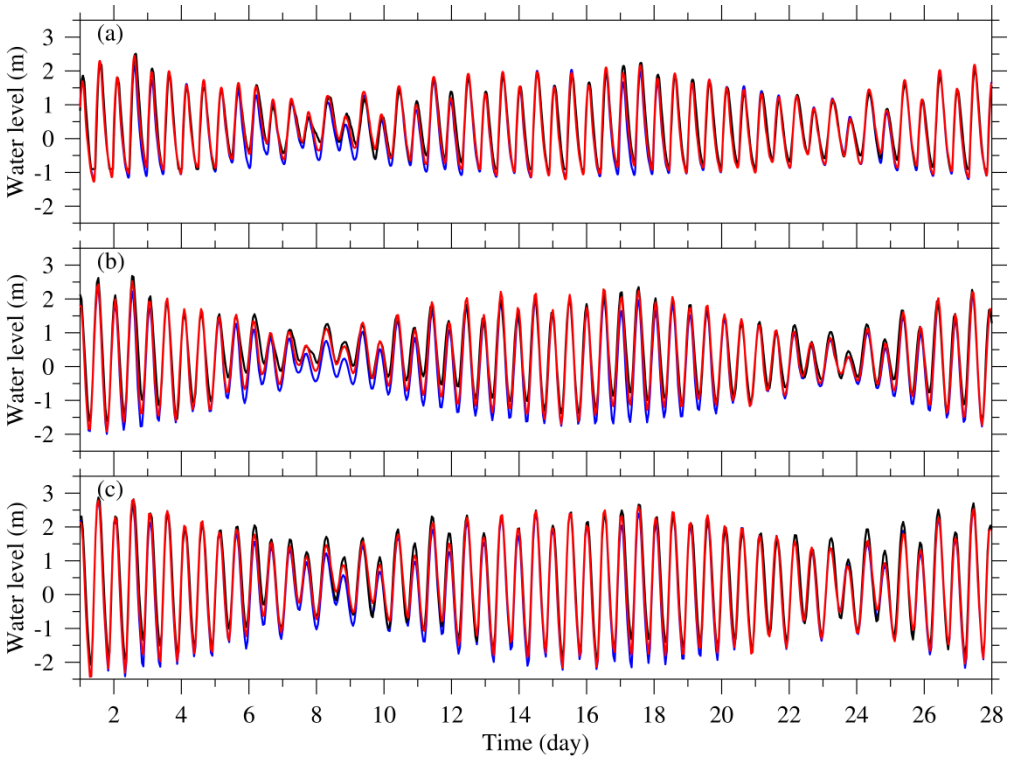

Figure 6: Temporal variations in water level in February 2014 at hydrologic stations. a: Baozhen station; b: Sheshan station; c: Luchaogang station. Black line: measured data; blue line: simulated data by Exp 1; red line: simulated data by Exp 2.

Comment 4: Section 4: In principle, the discussion part should systematically discuss the potential mechanism of saltwater intrusion with regard to the persistent and strong northerly wind. How the wind affects the individual terms in the momentum equation? The relationship between residual water level rise and wind? The generation of Ekman transport and the resulted horizontal circulation etc. In current form, the discussion part is more or less the same as the conclusions part since we see an identical sentence "With more frequent persistent and strong northerly wind caused by climate change, more attention should be paid to extremely severe saltwater intrusion events and freshwater safety in the Changjiang Estuary because the Qingcaosha Reservoir takes water from the Changjiang Estuary for the 13 million people in Shanghai" in both sections.

Reply: Thanks for your good suggestion. Now we added some numerical experiments and analyses in the discussion section to further reveal the potential mechanism of extremely severe saltwater intrusion in the revised manuscript. The

discussion 4 was rewritten as follows.

4 Discussion

In this section, the potential mechanism of the extremely severe saltwater intrusion with regard to the SSO, how the wind affects the individual terms in the momentum equations, relationship between residual water level rise and wind, generation of Ekman transport and the resulted horizontal circulation, and how long the northerly wind will induce severe saltwater intrusion were systematically discussed.

4.1 How much contribution the SSO had in the saltwater intrusion event?

The most feature of saltwater intrusion in the Changjiang Estuary is the SSO. Previous studies showed that the SSO is the main source of saltwater intrusion in the upper and middle reaches of the South Branch and the main saltwater source of the reservoirs (Shen et al. 2003; Wu et al. 2006; Zhu et al., 2013; Lyu and Zhu, 2018). How much contribution the SSO had in the extremely severe saltwater intrusion in February 2014? A transect Sec 2 at the upper reaches of the North Branch (location labelled in Fig. 1) was set to calculate water and salt flux.

In Exp 1, the water flux from February 6 to 8, 2014 and salt flux on February 7, 2014 was transported from the South Branch into the North Branch. This phenomenon was occurred in neap tide (indicated by the water level in Fig. 6), while in the other tidal patterns the water and salt flux was transported from the North Branch into the South Branch, especially during the spring tide from February 14 to 17, 2014. This is the SSO occurring during middle and spring tide in dry season.

In Exp 2, the seaward water flux on February 7 became smaller and the landward water flux became larger from February 4 to 6 and from February 8 to 14, and the salt flux from February 4 to 14 was landward, under strong northerly wind, which was distinctly larger than the result under climatic wind and residual water level conditions at open sea boundaries. Therefore, the strong northerly wind enhanced the SSO, but was not the cause of the extremely severe saltwater intrusion event.

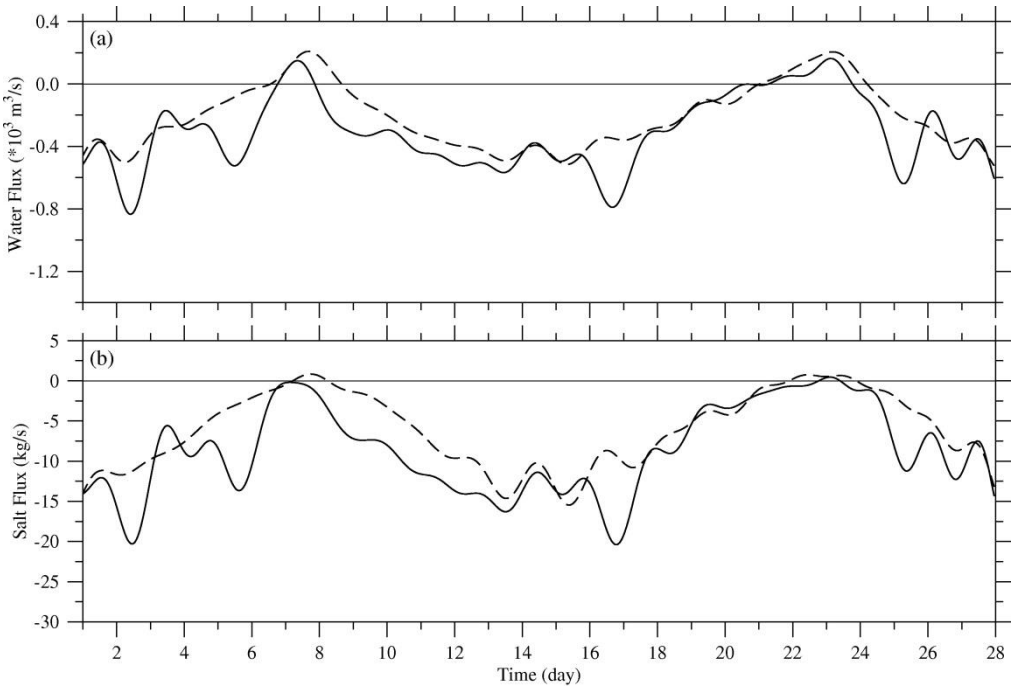

Figure 10: Temporal variations in residual water flux (a) and salt flux (b) across Sec 2 at the North Branch in February 2014. Dashed line: Exp 1; solid line: Exp 2. A positive value represents seaward flux, and a negative value represents landward flux.

A numerical experiment was designed in which the upper reaches of the North Branch is blocked (location labelled in Fig. 1) to further distinguish the contribution of SSO in the saltwater intrusion event. The distribution of time-averaged surface salinity from February 10 to 13, 2014 (Fig. 11a) and the temporal variations in salinity from February 8 to 22, 2014 at Chongxin station (Fig. 11b) show that the SSO was completely disappeared, while the salinity in the river mouth and near the Qingcaosha reservoir, and at the Baozhen, Nanmen and Qingcaosh stations were almost same as the results with Exp 2 (Fig. 7d, Fig. 3), indicating that the SSO almost had no contribution in the saltwater intrusion event in February 2014.

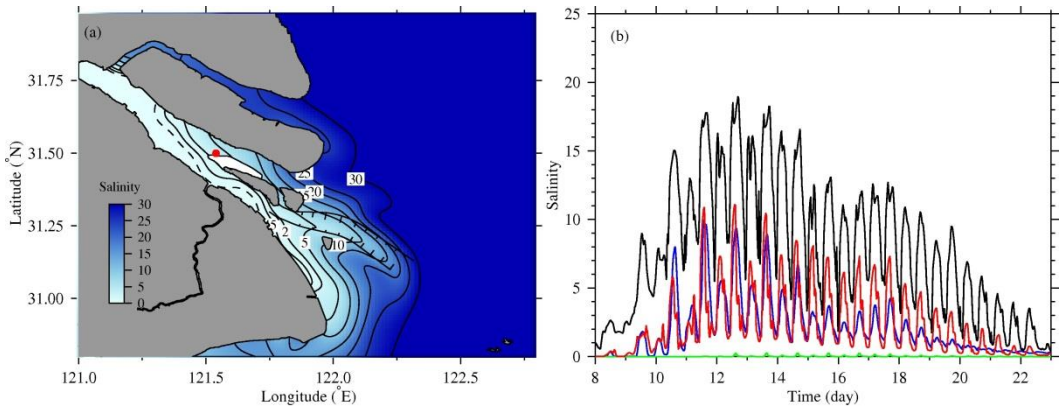

Figure 11: Distribution of time-averaged surface salinity from February 10 to 13, 2014 (a); and temporal variations in salinity from February 8 to 22, 2014 at hydrologic stations (b) if the upper reaches of the North Branch is blocked, and under a realistic wind and residual water levels at the open sea boundaries. Black line: Baozhen; red line: Nanmen; green line: Chongxi; blue line: Qingcaosha.

4.2 How the wind affects the individual terms in the momentum equations?

The modelled individual terms in the momentum equations were output at site Mo in the North Channel (labelled in Fig. 1, water depth 9.62 m) to analyse how the wind affects them. The momentum along the river channel (ξdirection) is:

$$\frac{\partial u}{\partial t} = -\frac{\partial u^2}{\partial \xi} - \frac{\partial uv}{\partial \eta} - \frac{\partial wu}{D\partial \sigma} + vf - \mathrm{g}\frac{\partial \zeta}{\partial \xi} + \frac{g}{\rho_0}\frac{\partial D}{\partial \xi}\int_\sigma^0 \sigma \frac{\partial \rho}{\partial \sigma} d\sigma - \frac{gD}{\rho_0}\frac{\partial}{\partial \xi}\int_\sigma^0 \rho d\sigma + \frac{1}{D^2}\frac{\partial}{\partial \sigma}\left(K_m \frac{\partial u}{\partial \sigma}\right) + F_\xi$$

And cross the river channel (ηdirection) is:

$$\frac{\partial v}{\partial t} = -\frac{\partial uv}{\partial \xi} - \frac{\partial v^2}{\partial \eta} - \frac{\partial wv}{D\partial \sigma} - uf - \mathrm{g}\frac{\partial \zeta}{\partial \eta} + \frac{g}{\rho_0}\frac{\partial D}{\partial \eta}\int_\sigma^0 \sigma \frac{\partial \rho}{\partial \sigma} d\sigma - \frac{gD}{\rho_0}\frac{\partial}{\partial \eta}\int_\sigma^0 \rho d\sigma + \frac{1}{D^2}\frac{\partial}{\partial \sigma}\left(K_m \frac{\partial v}{\partial \sigma}\right) + F_\eta$$

where, $\frac{\partial u}{\partial t}$ and $\frac{\partial v}{\partial t}$ is the local variation, $-\frac{\partial u^2}{\partial \xi} - \frac{\partial uv}{\partial \eta} - \frac{\partial wu}{D\partial \sigma}$ and $-\frac{\partial uv}{\partial \xi} - \frac{\partial v^2}{\partial \eta} - \frac{\partial wv}{D\partial \sigma}$ is advection, vf and $-uf$ is Coriolis force, $-\mathrm{g}\frac{\partial \zeta}{\partial \xi}$ and $-\mathrm{g}\frac{\partial \zeta}{\partial \eta}$ is barotropic pressure gradient force, $\frac{g}{\rho_0}\frac{\partial D}{\partial \xi}\int_\sigma^0 \sigma \frac{\partial \rho}{\partial \sigma} d\sigma - \frac{gD}{\rho_0}\frac{\partial}{\partial \xi}\int_\sigma^0 \rho d\sigma$ and $\frac{g}{\rho_0}\frac{\partial D}{\partial \eta}\int_\sigma^0 \sigma \frac{\partial \rho}{\partial \sigma} d\sigma - \frac{gD}{\rho_0}\frac{\partial}{\partial \eta}\int_\sigma^0 \rho d\sigma$ is baroclinic pressure gradient force, $\frac{1}{D^2}\frac{\partial}{\partial \sigma}\left(K_m \frac{\partial u}{\partial \sigma}\right)$ and $\frac{1}{D^2}\frac{\partial}{\partial \sigma}\left(K_m \frac{\partial v}{\partial \sigma}\right)$ is vertical turbulence viscosity, $F_\xi$and F_η is horizontal turbulence viscosity, in $\xi$and η direction, respectively. Each output term in the momentum equations was vertically averaged, and the vertical turbulence viscosity $\frac{1}{D^2}\frac{\partial}{\partial \sigma}\left(K_m \frac{\partial u}{\partial \sigma}\right)$ and $\frac{1}{D^2}\frac{\partial}{\partial \sigma}\left(K_m \frac{\partial v}{\partial \sigma}\right)$ equals $\frac{\tau_{a\xi} - \tau_{b\xi}}{D}$, $\frac{\tau_{a\eta} - \tau_{b\eta}}{D}$, in which $\tau_{a\xi}$, $\tau_{a\eta}$ and $\tau_{b\xi}$, $\tau_{b\eta}$ is wind stress and bottom friction force in ξ and η direction, respectively. The tidal fluctuations in the vertically averaged terms were filtered by moving average method.

In Exp 1, the residual water movement along the North Channel was mainly determined by the seaward barotropic pressure gradient force and Coriolis force (Fig.

12a). The residual barotropic pressure gradient force was positive (seaward) induced mainly by river discharge, and varies with tide, had a smaller value from February 7 to 9, 2014 (in neap tide, Fig. 6). The seaward runoff produced a negative Coriolis force. The baroclinic pressure gradient force was very small before February 10 because the saltwater intrusion was very weak at the model output site, then became larger with the increase of tide. This term always is landward in estuary because the saline water is downstream. Across the channel, the residual water movement was also mainly determined by the seaward barotropic pressure gradient force and Coriolis force (Fig. 12b). The barotropic pressure gradient force was positive (northward) because the water level is higher on south side of the channel than on north side due to the effect of the Coriolis force on runoff. The baroclinic pressure gradient force was negative because salinity was higher on the north side than on the south side due to the effect of the Coriolis force on the flood current that brought saline water into the estuary.

In Exp 2, the situation in Exp 1 was changed greatly (Fig. 12c, d). The persistent and strong wind induced larger southward wind stress (red solid line in Fig. 12d), produced landward Ekman transport and water level rise, which significantly reduced the seaward barotropic pressure gradient force, especially from February 7 to 8, 2014. At this time, the barotropic pressure gradient force was very small, even negative (landward), that made the net water transport landward, greatly enhancing the saltwater intrusion in the North Channel, meanwhile distinctly increasing the landward baroclinic pressure gradient force (black dashed line in Fig. 12c).

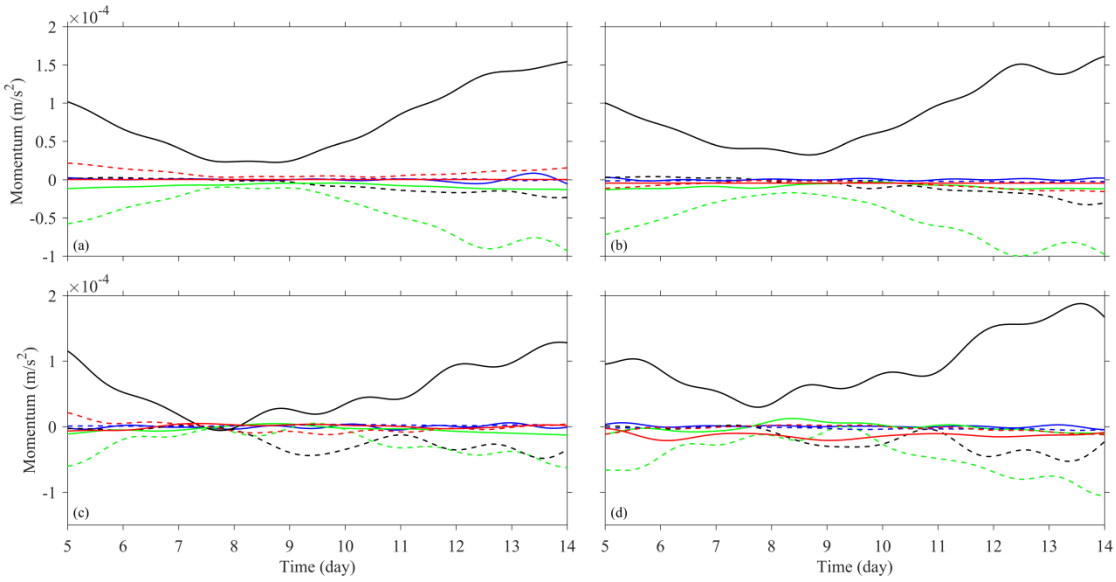

Figure 12: Temporal variations in the vertically and time averaged terms in the momentum equations along the channel (left panel, a and c) and across the channel (right panel, b and d) from February 5 to 13, 2014 in Exp 1 (upper panel) and Exp 2 (lower panel) at site Mo in the North Channel. Red solid line: wind stress at river surface; red dashed line: bottom friction force; black solid line: barotropic pressure gradient force; black dashed line: baroclinic pressure gradient force; green solid line: Coriolis force; green dashed line: advection; blue solid line: local variation; blue dashed line: horizontal turbulence viscosity.

4.3 The relationship between residual water level rise and wind

The water level rise in the Changjiang Estuary is closely related with the wind. The water level at Sheshan and Luchaogang station rose during northerly wind and dropped during southerly wind in February 2014 (Fig. 4b, c and d). High water level rise of more than 50 cm corresponded to the strong northerly wind. The water level is approximately 20 cm (Fig. 5b) under climatic wind in February and 30 cm (Fig. 9b) under persistent and strong northerly wind in February 2014. At Baozhen, Sheshan and Luchaogang station in February 2014, the modelled water level under climatic wind is lower than the one under strong northerly wind, especially from February 6 to 10, 2014, the difference reached 10~30 cm (Fig. 6). Therefore, the stronger the northerly wind is, the higher the water level in the Changjiang estuary and adjacent sea rises.

4.4 The generation of Ekman transport and the resulted horizontal circulation

The northerly wind produces southward current along the China coast, and push

water landward transport by Coriolis force, resulting in water level rise along the coast. In the Changjiang Estuary, this dynamic mechanism causes a pure wind-driven horizontal circulation that flows into the North Channel and out of the South Channel (Fig. 13a). The wind-driven estuarine current can enhance saltwater intrusion in the North Channel, and weaken it in the South Channel. Previous studies revealed the dynamic mechanism of northerly wind on the saltwater intrusion by the pure wind-driven current in the estuary (Wu et al., 2010; Li et al, 2012). In this study, the horizontal estuarine circulation was a total (net) circulation induced by the river discharge, tide and persistent and strong northerly wind (Fig. 9c), was not a pure wind-driven circulation, which surpassed the strong seaward runoff from February 9 to 13, 2014 (Fig. 8a). This result was unexpected and surprising, and was found for the first time.

A numerical experiment was set up with different northerly wind speed to ascertain how much wind can make the water flux at sec1 in the North Channel landward transport. Except for the wind, the other dynamic factors are the same as in Exp 2. The results is that the net water flux is seaward when wind is less than 8 m/s, is approximately zero when wind speed is 10 m/s, and landward when wind speed is larger than 10 m/s (Fig. 13b). The landward water flux enhances with increase of northerly wind. Therefore, northerly wind with speed of more than 10 m/s can called strong wind that causes net water transport landward in the North Channel.

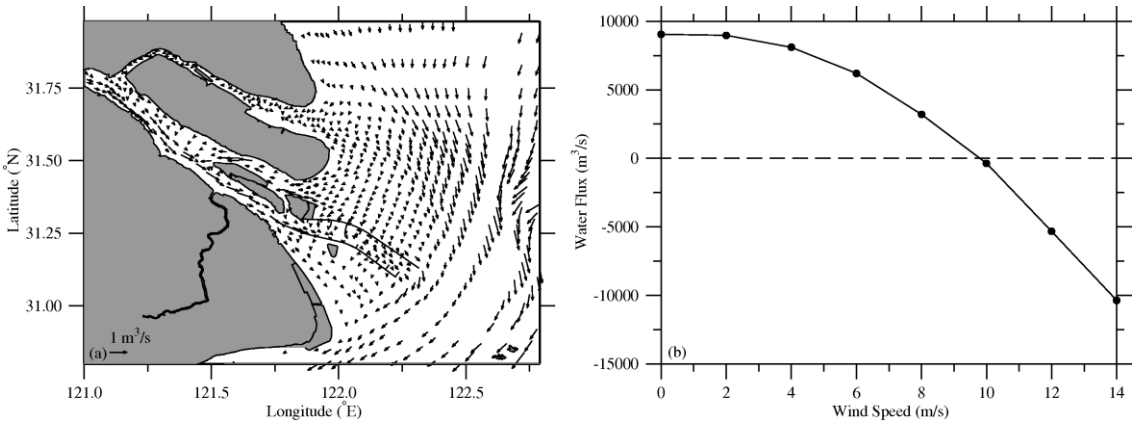

Figure 13: Distribution of pure wind-driven current time-averaged from February 10 to 13, 2014 modelled under the real wind (a). Relationship between water flux across sec1 in the North Channel and northerly wind speed (b). Except for the wind, the other dynamic factors are the same

as in Exp 2.

4.5 How long the northerly wind will induce severe saltwater intrusion?

In winter, there are frequent cold fronts passing over the Changjiang Estuary and bringing strong northerly winds, enhancing saltwater intrusion (Li et al., 2012). For example, the relatively stronger saltwater intrusions occurred from February 15 to 18, 2011, and from February 23 to 26, 2017 were caused by the passing cold fronts. No extremely severe saltwater intrusion event occurred because the strong northerly wind induced by the cold fronts lasted only 1-2 days. How long the northerly wind will induce severe saltwater intrusion? Based on the persistent and strong northerly wind process in February 2014, numerical experiments were conducted, and the results indicate that if a strong northerly wind lasts 2 days, saltwater intrusion is weak (Fig. 14), which is similar to the case of an ordinary cold front passage; if a strong northerly wind lasts 4 days, saltwater intrusion is stronger than normal, similar to the case of a stronger cold front passage. It can been seen that 4 days strong wind can induce the higher than normal salinity in after 8 days, because the strong wind Ekman transport brought the salinity front in the sandbar area upstream and closer to the Baozhen station, and then move upstream and downstream with the oscillation of flood and ebb current for 8 days after the strong northerly wind became northerly wind with speed of 5 m/s. If a strong northerly wind lasts 6 days, saltwater intrusion becomes severe; if a strong northerly wind lasts 8 days, the salinity is dramatically increased, the maximum salinity approaches the real salinity, and the saltwater intrusion becomes extremely severe. Therefore, the longer the strong northerly wind lasts, the more severe the saltwater intrusion is.

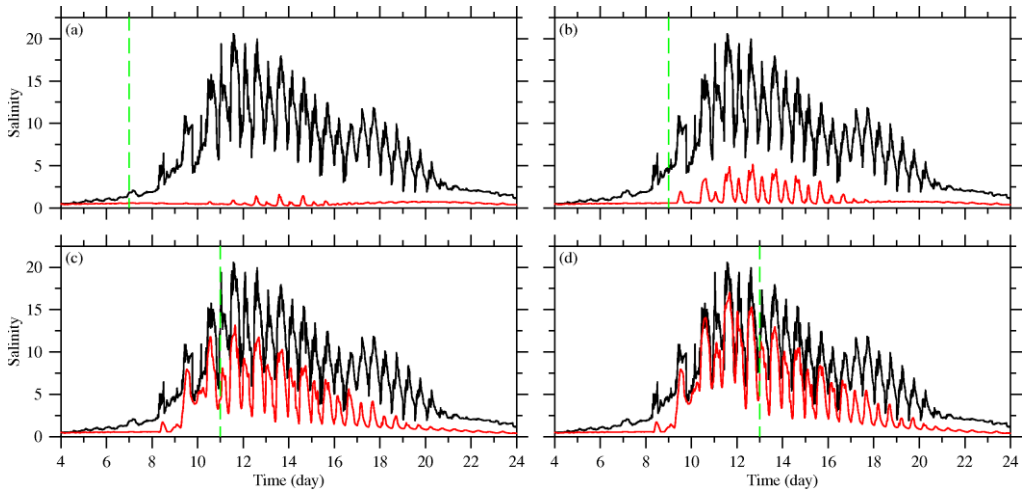

Figure 14: Temporal variation in observed (black line) and modelled (red line) salinity at Baozhen station from February 4 to 24, 2014. The green dashed lines indicate the time before it the wind was realistic and after it was set to 5 m s^{-1}.

The sentence “With more frequent persistent and strong northerly wind caused by climate change, more attention should be paid to extremely severe saltwater intrusion events and freshwater safety in the Changjiang Estuary because the Qingcaosha Reservoir takes water from the Changjiang Estuary for the 13 million people in Shanghai” in the discussion section was removed in the revised manuscript.

The contents added in discussion section were embodied in the conclusion section.

Other figures in the revised manuscript are listed follows.

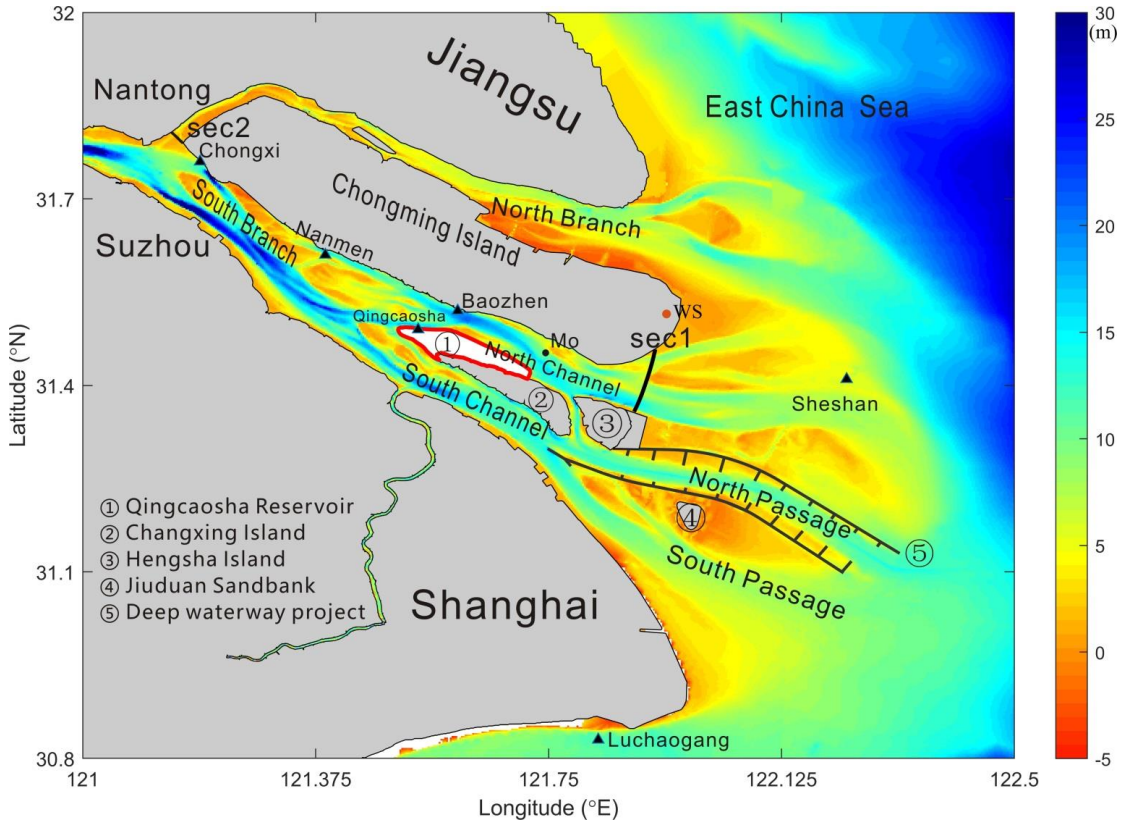

Figure 1: Topography of the Changjiang Estuary. The black triangles indicate the locations of hydrologic stations Chongxi, Nanmen, Baozhen, Qingcaosha, Sheshan and Luchaogang. The WS is the location of the weather station at the Chongming eastern shoal. sec1 and sec2 is a transect at the river mouth of the North Channel and upper reaches of the North Branch, and Mo is the model output site for terms in the momentum equations.

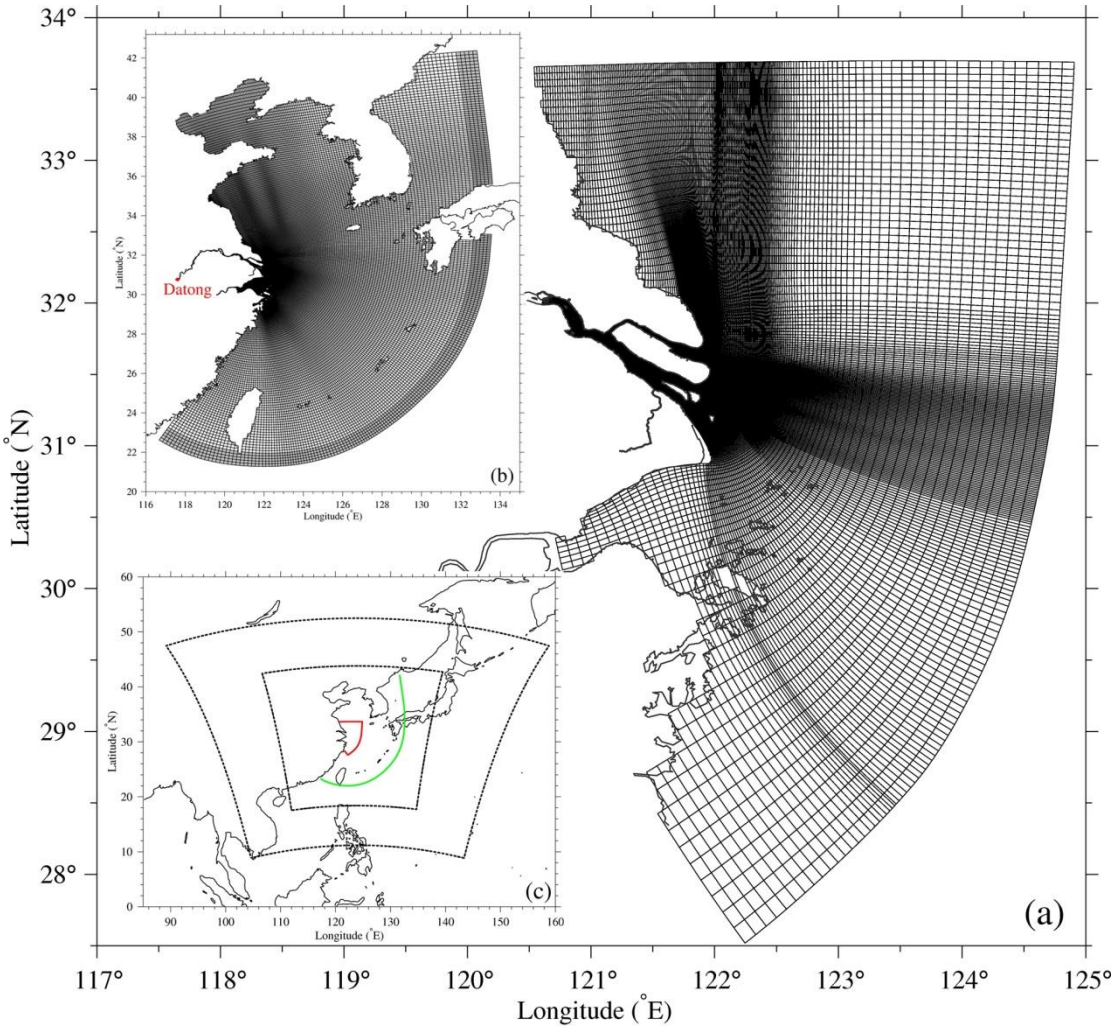

Figure 2: Model grids of the Changjiang Estuary (a), and model grids of the Bohai Sea, Yellow Sea and East China Sea (b). Domains of the models (c); within the red line: the Changjiang Estuary model domain; within the green line: model domain of the Bohai Sea, Yellow Sea and East China Sea; the black dashed lines: the two-fold nested WRF model domain

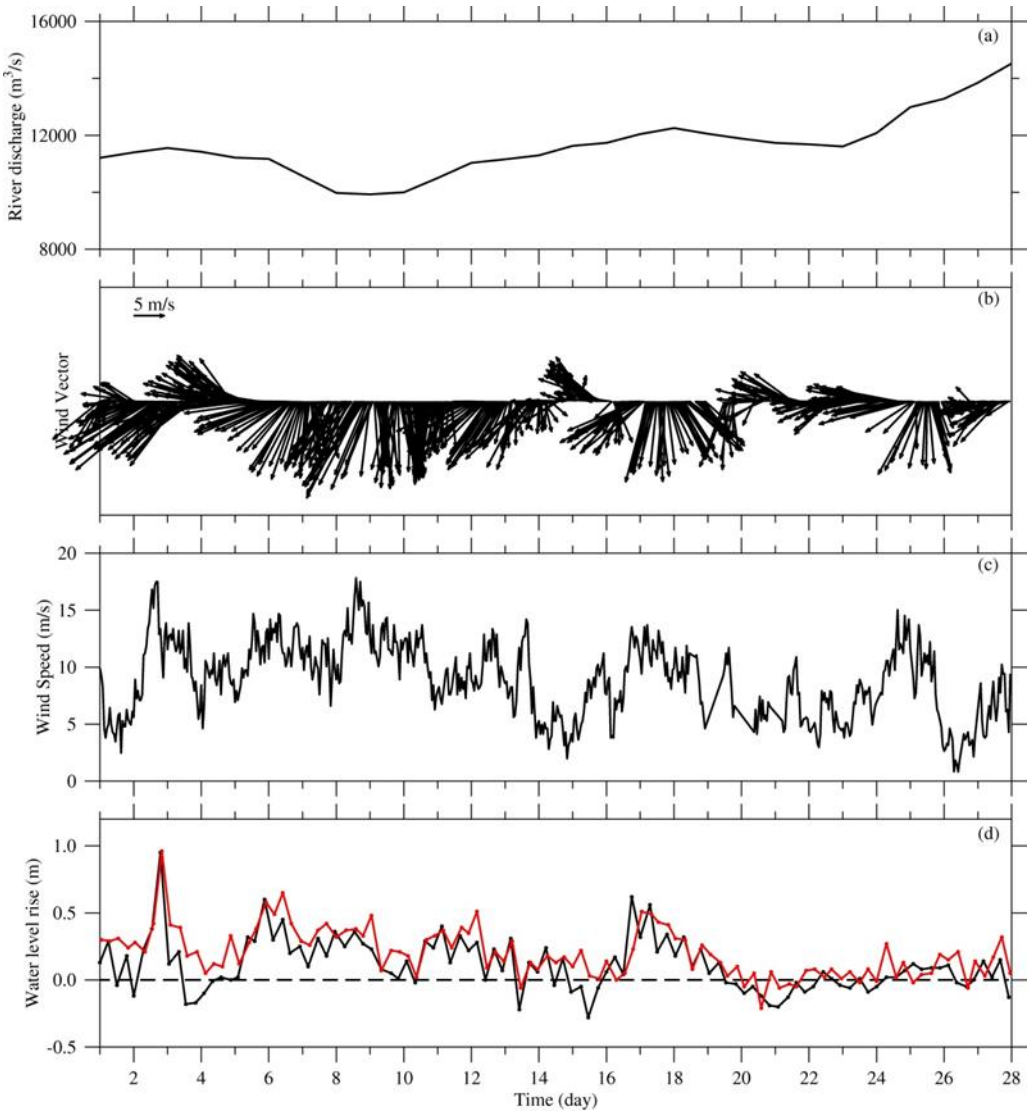

Figure 4: Temporal variations in the measured river discharge at Datong station (a), wind vector (b) and wind speed (c) at WS, and water level rise obtained by subtracting the data in the tide table from the measured water level at Sheshan station (black line) and Luchaogang station (red line) (d) in February 2014.

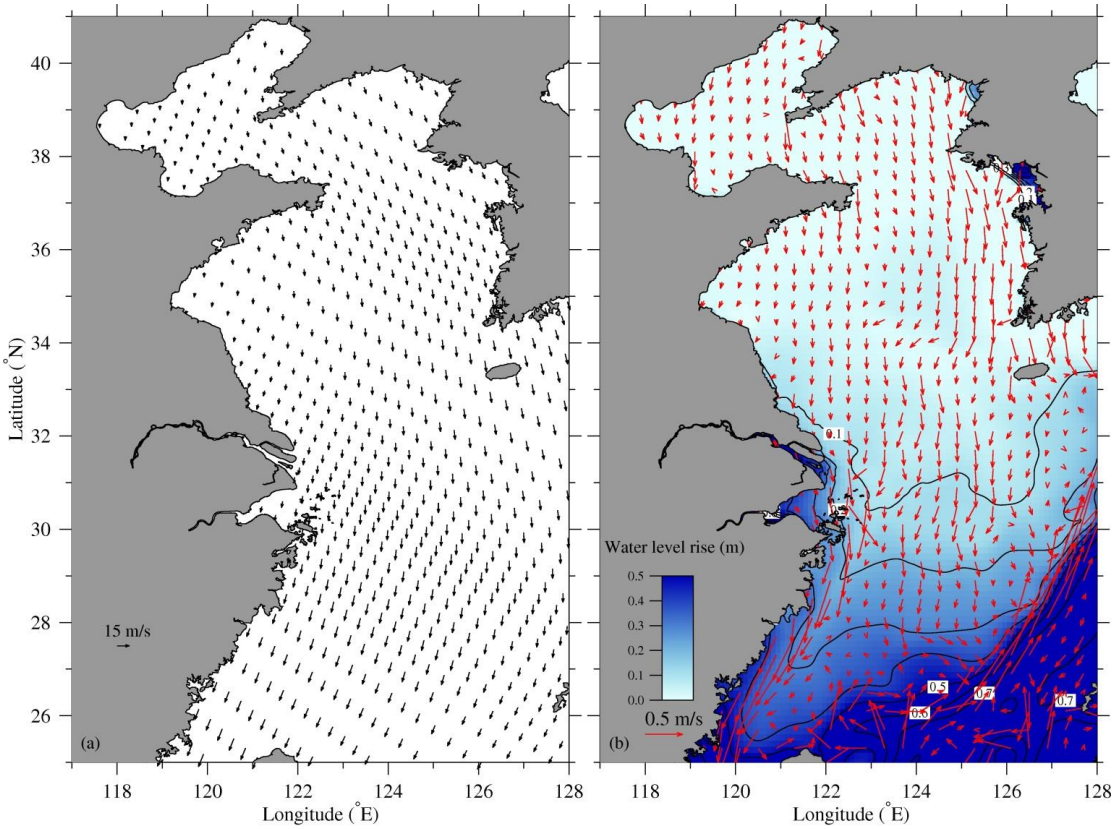

Figure 5: Distributions of the climatic wind field (a), and residual water level and surface current (b) in February.

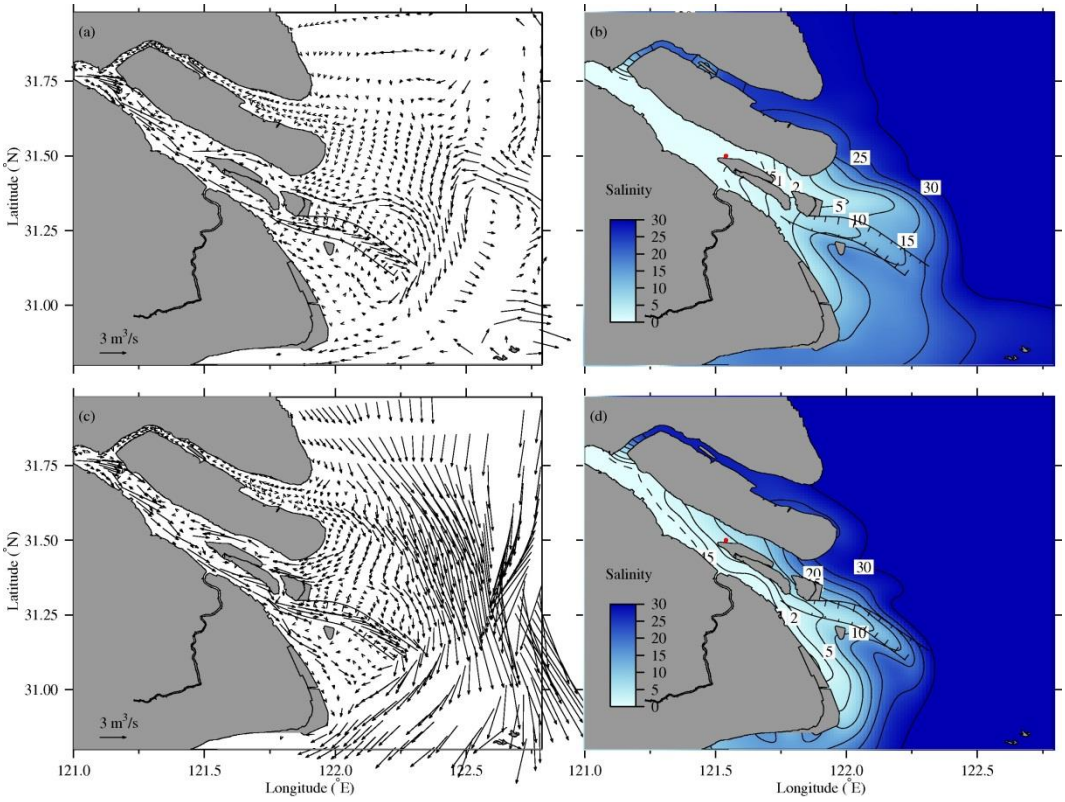

Figure 7: Distributions of residual unit width water flux (a, c) and time-averaged surface salinity (b, d) from February 10 to 13, 2014 by Exp 1 (upper panel) and Exp 2 (lower panel). The dashed isohaline represents a salinity of 0.45; the red dot denotes the location of water intake for Qingcaosha Reservoir (similarly hereinafter).

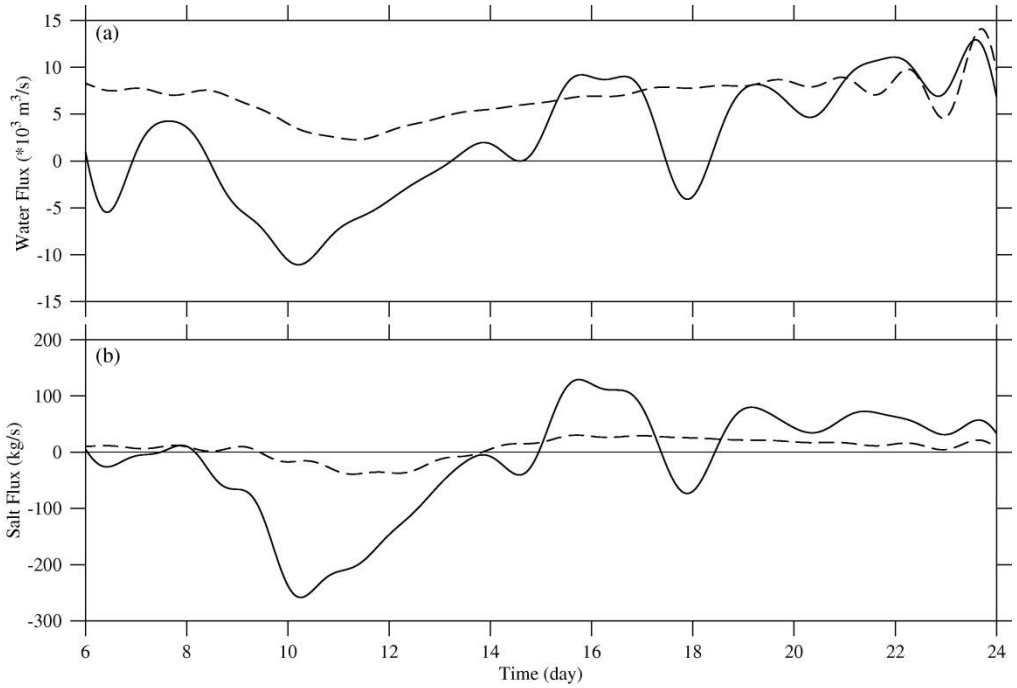

Figure 8: Temporal variations in residual water flux (a) and salt flux (c) across Sec 1 in the North Channel from February 6 to 24, 2014. Dashed line: Exp 1; solid line: Exp 2. A positive value represents seaward flux, and a negative value represents landward flux.

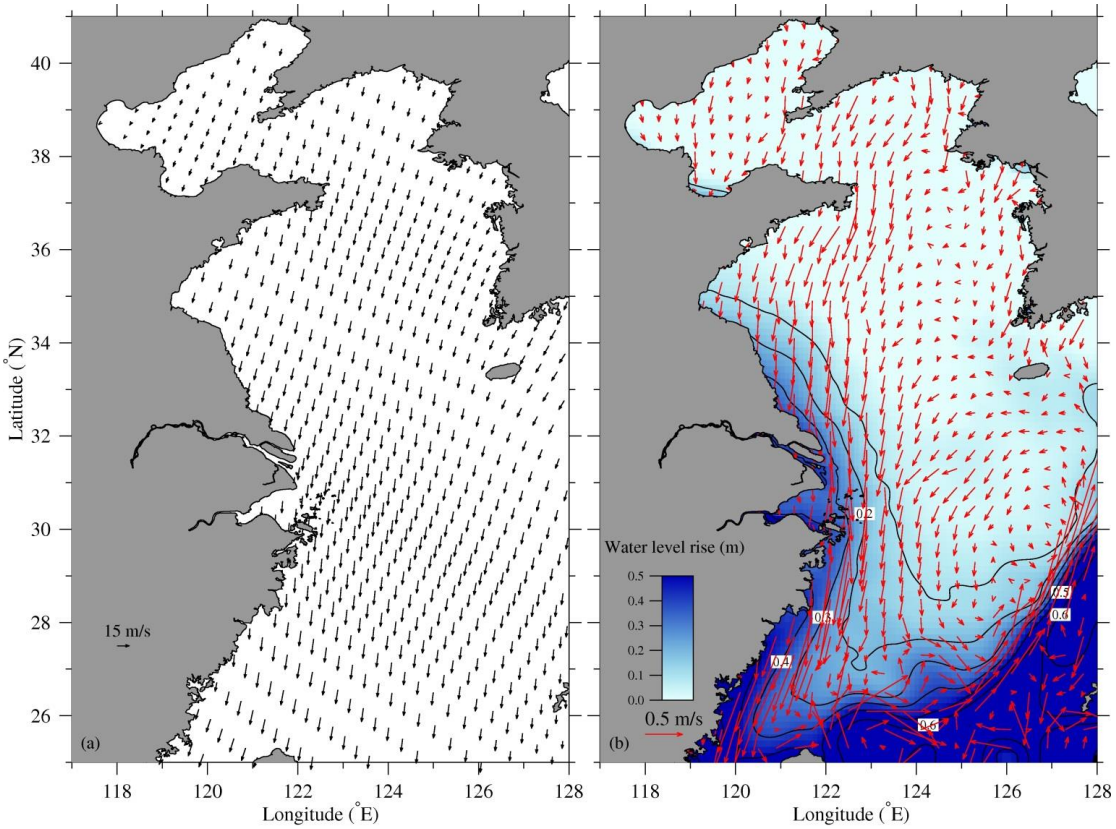

Figure 9: Distributions of the temporally averaged wind field from February 7 to 14, 2014, as simulated by the WRF model (a), and the time-averaged water level and surface current from February 10 to 13, 2014, as simulated by the model encompassing the Bohai Sea, Yellow Sea and East China Sea (b).